

Electronic Supplementary Information (ESI) for

Silver vanadium oxide@water-pillared vanadium oxide coaxial nanocables for superior zinc-ion storage properties

Jing Zeng^{†,a} Kun Chao^{†,b} Wenquan Wang,^a Xin Wei,^a Chenyang Liu,^a Hongrui Peng,^a Zhonghua Zhang,^a Xiaosong Guo^{*a} and Guicun Li^{*a}

^aCollege of Materials Science and Engineering, Qingdao University of Science and Technology, Qingdao 266042, China

^bCollege of Electromechanical Engineering, Qingdao University of Science and Technology, Qingdao 266042, China

E-mail: guicunli@qust.edu.cn, guoxs06@126.com

This profile contains following contents.

Fig. S1 TEM images of the $\text{Ag}_{0.333}\text{V}_2\text{O}_5@V_2\text{O}_5 \cdot n\text{H}_2\text{O}$ coaxial nanocables.

Fig. S2 TEM and HRTEM images of $V_2\text{O}_5/V_2\text{O}_5 \cdot n\text{H}_2\text{O}$ (a and b) and $\text{Ag}_{0.333}\text{V}_2\text{O}_5$ (c and d).

Fig. S3 TEM-EDS image of the elemental distributions of O in $\text{Ag}_{0.333}\text{V}_2\text{O}_5@V_2\text{O}_5 \cdot n\text{H}_2\text{O}$.

Fig. S4 EDS spectrum of the $\text{Ag}_{0.333}\text{V}_2\text{O}_5@V_2\text{O}_5 \cdot n\text{H}_2\text{O}$ coaxial nanocables.

Table S1 The detailed analysis data in XPS experiments for varied elements.

Fig. S5 The first cycle discharge-charge profiles of (a) $\text{Ag}_{0.333}\text{V}_2\text{O}_5@V_2\text{O}_5 \cdot n\text{H}_2\text{O}$; (b) $\text{Ag}_{0.333}\text{V}_2\text{O}_5$; and (c) $V_2\text{O}_5/V_2\text{O}_5 \cdot n\text{H}_2\text{O}$.

Fig. S6 Nyquist impedance plots of varied electrodes fresh cells.

Fig. S7 Discharge–charge curves of the $\text{Ag}_{0.333}\text{V}_2\text{O}_5@V_2\text{O}_5 \cdot n\text{H}_2\text{O}$ cathode at different current densities.

Fig. S8 SEM images of $\text{Ag}_{0.333}\text{V}_2\text{O}_5@V_2\text{O}_5 \cdot n\text{H}_2\text{O}$ cathode after 100 cycles at 0.5 A g^{-1} .

Fig. S9 SEM images of initial $\text{Ag}_{0.333}\text{V}_2\text{O}_5@V_2\text{O}_5 \cdot n\text{H}_2\text{O}$ cathode (a and b); and after cycled $\text{Ag}_{0.333}\text{V}_2\text{O}_5@V_2\text{O}_5 \cdot n\text{H}_2\text{O}$ cathode (c and d); The insets in part a and c shows the status of the electrodes.

Fig. S10 The long-time cycling performance of the electrodes for comparison at 3.0 A g^{-1} .

Fig. S11 EDS images of the thick $\text{Ag}_{0.333}\text{V}_2\text{O}_5@V_2\text{O}_5 \cdot n\text{H}_2\text{O}$ electrode.

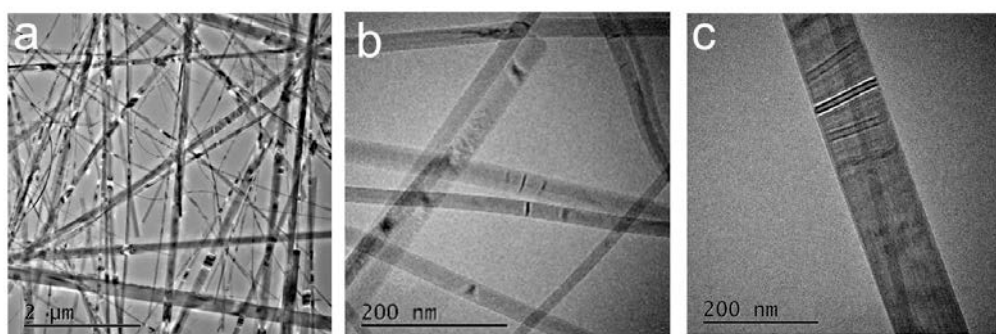


Fig. S1 TEM images (a,b and c) of the $\text{Ag}_{0.333}\text{V}_2\text{O}_5@V_2\text{O}_5 \cdot n\text{H}_2\text{O}$ coaxial nanocables.

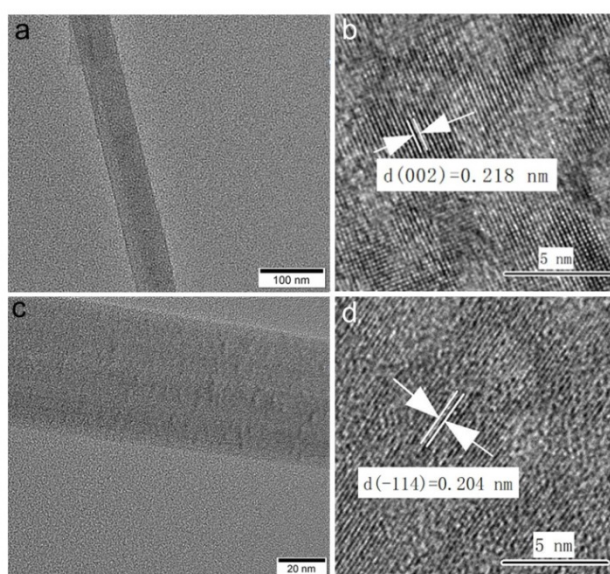


Fig. S2 Typical TEM and HRTEM images of $V_2\text{O}_5/V_2\text{O}_5 \cdot n\text{H}_2\text{O}$ (a and b) and $\text{Ag}_{0.333}\text{V}_2\text{O}_5$ (c and

d).

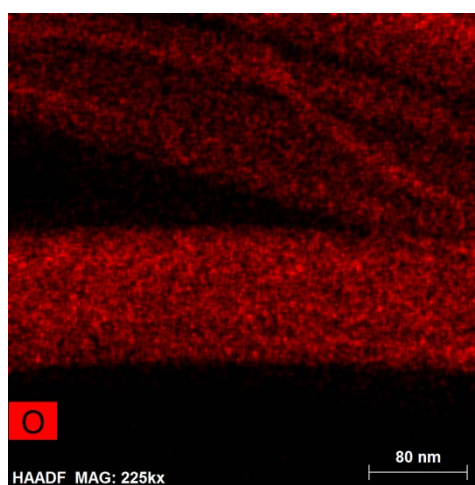


Fig. S3 TEM-EDS image of the elemental distributions of O in $\text{Ag}_{0.333}\text{V}_2\text{O}_5@ \text{V}_2\text{O}_5 \cdot n\text{H}_2\text{O}$.

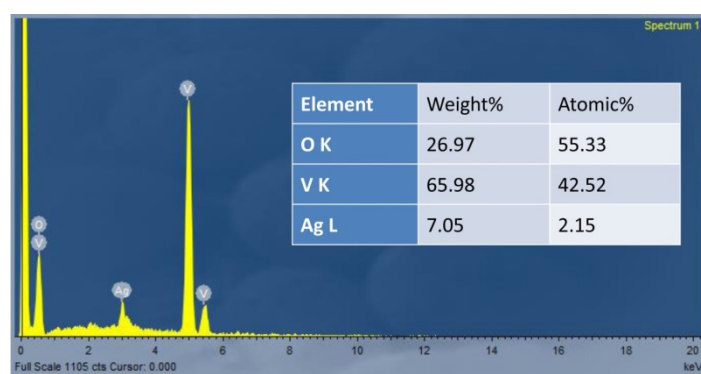


Fig. S4 EDS spectrum of the $\text{Ag}_{0.333}\text{V}_2\text{O}_5@ \text{V}_2\text{O}_5 \cdot n\text{H}_2\text{O}$ coaxial nanocables.

The EDS result demonstrated the atomic ratio of Ag to V is about 0.05, which is consistent with the results of XPS (Table S1).

Table S1 The detailed analysis data in XPS experiments for varied elements.

Name	Start BE	Peak BE	End BE	Height CPS	FWHM eV	Area (P) CPS.eV	Area (N) TPP-2M	Atomic %
C1s	293.83	284.79	280.83	10708.22	1.56	22954.87	0.29	23.92
Ag3d	378.48	367.82	364.23	10067.82	1.13	21629.04	0.01	1.05
V2p	528.78	517.58	512.68	57820.53	1.38	147450.9	0.22	17.92
O1s	543.98	530.41	527.88	72386.79	1.54	145134.67	0.69	57.11

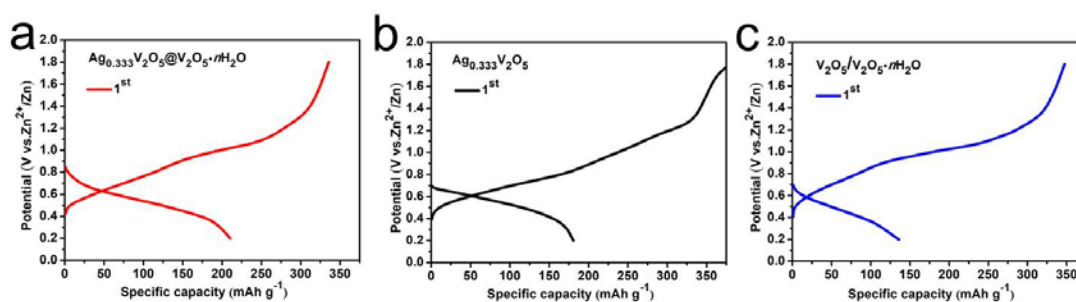


Fig. S5 The first cycle discharge-charge profiles of (a) $\text{Ag}_{0.333}\text{V}_2\text{O}_5@V_2\text{O}_5 \cdot n\text{H}_2\text{O}$; (b) $\text{Ag}_{0.333}\text{V}_2\text{O}_5$; and (c) $V_2\text{O}_5/V_2\text{O}_5 \cdot n\text{H}_2\text{O}$.

The first cycle discharge-charge specific capacity of $\text{Ag}_{0.333}\text{V}_2\text{O}_5@V_2\text{O}_5 \cdot n\text{H}_2\text{O}$ ($210.18 \text{ mAh g}^{-1}$ at 0.5 A g^{-1}), $\text{Ag}_{0.333}\text{V}_2\text{O}_5$ ($180.56 \text{ mAh g}^{-1}$ at 0.2 A g^{-1}), $V_2\text{O}_5/V_2\text{O}_5 \cdot n\text{H}_2\text{O}$ ($135.03 \text{ mAh g}^{-1}$ at 0.2 A g^{-1}) are shown in Fig. S4, respectively.

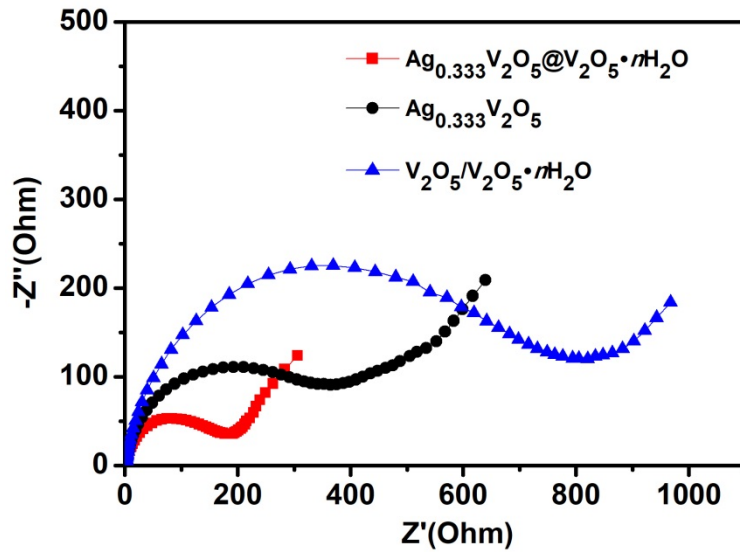


Fig. S6 Nyquist impedance plots of varied electrodes fresh cells.

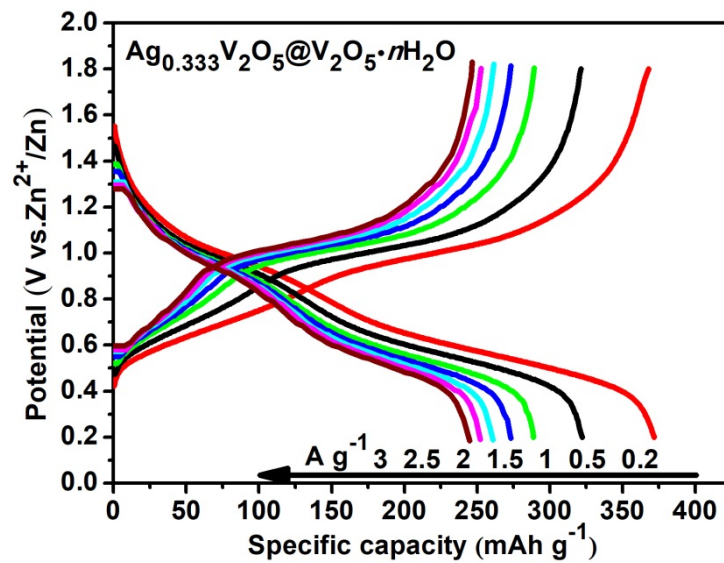


Fig. S7 Discharge-charge curves of the $\text{Ag}_{0.333}\text{V}_2\text{O}_5@V_2\text{O}_5 \cdot n\text{H}_2\text{O}$ cathode at different current densities.

The discharge-charge curves of the $\text{Ag}_{0.333}\text{V}_2\text{O}_5@V_2\text{O}_5 \cdot n\text{H}_2\text{O}$ cathode at different current densities shows in Fig. S6. The charge-discharge curves features are kept well, even in a higher current density of 3.0 A g^{-1} . The specific capacities $373.3, 322.5, 290.62, 274.18, 262.72, 253.76$ and 245.9 mAh g^{-1} are obtained at $0.2, 0.5, 1.0, 1.5, 2.0, 2.5$ and 3.0 A g^{-1} , respectively.

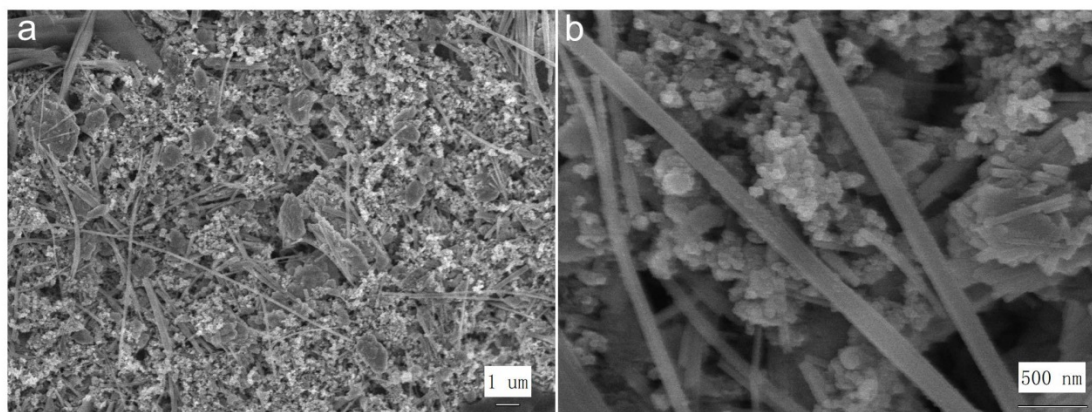


Fig. S8 SEM images of $\text{Ag}_{0.333}\text{V}_2\text{O}_5@V_2\text{O}_5 \cdot n\text{H}_2\text{O}$ cathode after 100 cycles at 0.5 A g^{-1} .

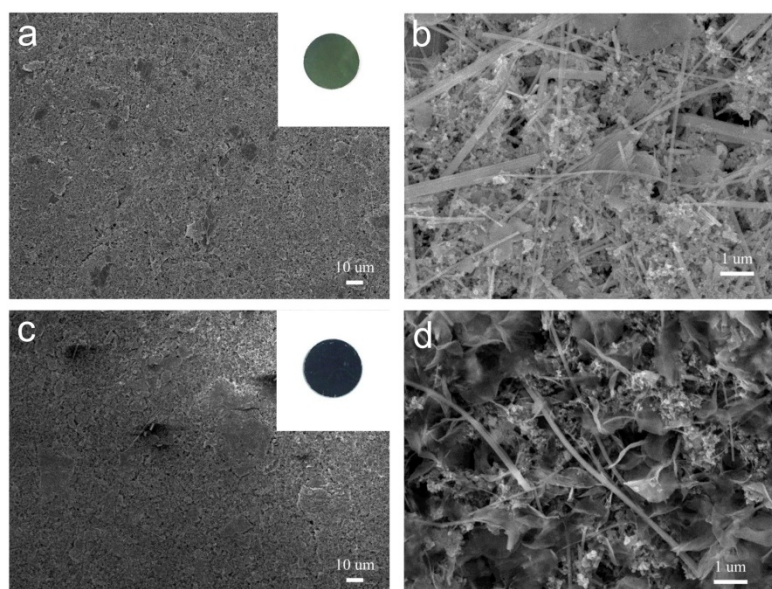


Fig. S9 SEM images of initial $\text{Ag}_{0.333}\text{V}_2\text{O}_5@V_2\text{O}_5 \cdot n\text{H}_2\text{O}$ cathode (a and b); and after cycled $\text{Ag}_{0.333}\text{V}_2\text{O}_5@V_2\text{O}_5 \cdot n\text{H}_2\text{O}$ cathode (c and d); The insets in part a and c shows the status of the electrodes.

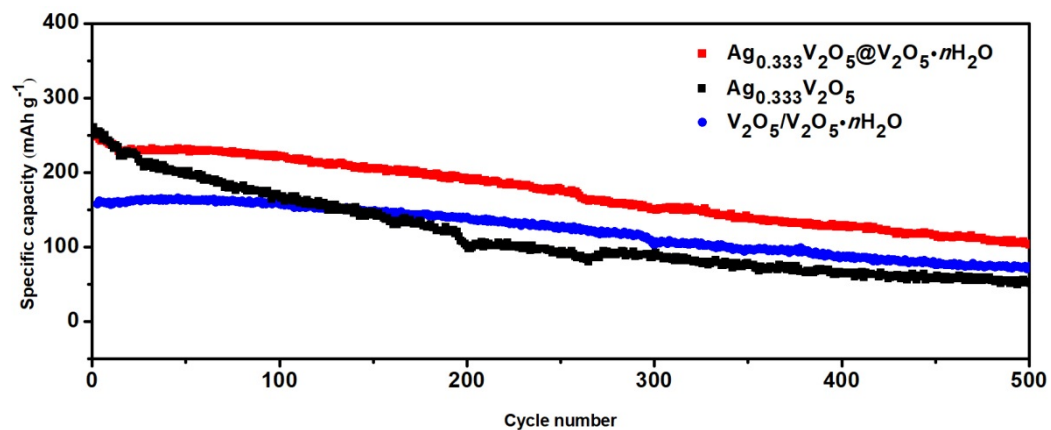


Fig. S10 The long-term cycling performance of the electrodes for comparison at 3.0 A g^{-1} .

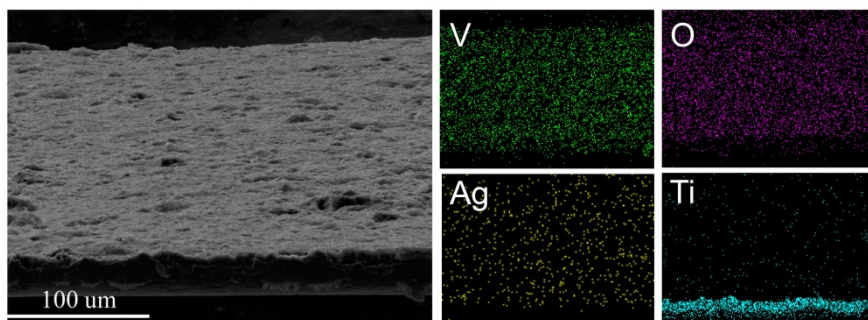


Fig. S11 EDS images of the thick $\text{Ag}_{0.333}\text{V}_2\text{O}_5@V_2\text{O}_5 \cdot n\text{H}_2\text{O}$ electrode.